A&A 444, L25–L28 (2005)
DOI: 10.1051/0004-6361:200500200

Astronomy & Astrophysics

Letter to the Editor

Roche lobe sizes in deep-MOND gravity

Hong Sheng Zhao

SUPA, School of Physics and Astronomy, University of St Andrews, KY16 9SS, Fife, UK⋆
National Astronomical Observatories, Chinese Academy of Sciences, Beijing 100012, PR China⋆⋆
e-mail: hz4@st-and.ac.uk

Received 3 May 2005 / Accepted 7 October 2005

ABSTRACT

MOdified Newtonian Dynamics survived the test over two decades, fitting the ups and downs of a variety of galaxy velocity curves without fine tuning (Sanders & McGaugh 2002, ARA&A, 40, 263). MOND is also evolving from an empirical to a decent theory respecting fundamental physics after Bekenstein (2004, Phys. Rev. D, 70, 3509) showed that lensing and Hubble expansion can be modeled rigourously in a Modified Relativity. However, many properties of MOND are obscured by its non-linear Poisson's equation. Here we study the effect of tides for a binary stellar system or a baryonic satellite-host galaxy system. We show that the Roche lobe is more squashed than the Newtonian case due to the anisotropic dilation effect in deep-MOND. We prove analytically that the Roche lobe volume scales linearly with the "true" baryonic mass ratio in both Newtonian and deep-MOND regimes, insensitive to the modification to the inertia mass. Hence accurate Roche radii of satellites can break the degeneracy of MOND and dark matter theory. Globular clusters and dwarf galaxies of comparable luminosities and distances show a factor of ten scatter in limiting radii; this is difficult to explain in any "mass-tracing-light" universe.

Key words. dark matter – galaxy kinematics and dynamics – gravitation – galaxies: dwarf – globular clusters

1. Introduction

The alternative gravity theory of Modified Newtonian Dynamics (MOND) (Milgrom 1983) has been doing very well in fitting kinematic data on galaxy scales, often better than the standard cold dark matter theory. Baryonic matter alone is sufficient to account for the gravity in such theory. The predictive power of this 20-year-old classical theory with virtually no free parameters (Bekenstein & Milgrom 1984) is recently highlighted by the astonishingly good fits to contemporary kinematic data of a wide variety of high and low surface brightness spiral and elliptical galaxies; even the fine details of the ups and downs of velocity curves are elegantly reproduced without fine tuning of the baryonic model (Sanders & McGaugh 2002; Milgrom & Sanders 2003). Originally it was proposed empirically (Milgrom 1983) that rotation curves of axisymmetric disk galaxies could be fit by an acceleration $g \equiv |\boldsymbol{g}| = V^2/r$ which is stronger than the Newtonian gravity GM/r^2 by a spatially varying factor $1/\mu$ in the weak regime defined by $g \leq a_0 \sim 1.2 \times 10^{-8}\,\mathrm{cm\,s^{-2}}$; e.g., $\mu(g/a_0) = \min(1, g/a_0) \leq 1$. This empirical MOND relation can be elevated to a theory for an arbitrary baryon density distribution $\rho(\boldsymbol{R})$, where a curl-free gravity field $\boldsymbol{g} = -\boldsymbol{\nabla}\Phi$ is the gradient of a conservative potential $\Phi(\boldsymbol{R})$ and satisfies an equation (Bekenstein & Milgrom 1984)

$$\boldsymbol{\nabla}\cdot\left[\frac{\mu\boldsymbol{g}}{4\pi G}\right] = -\rho(\boldsymbol{R}) \qquad \leftarrow \qquad \boldsymbol{\nabla}\cdot\frac{\epsilon\boldsymbol{E}}{4\pi} = -e(\boldsymbol{R}). \tag{1}$$

Here we made the analogy with the Poisson's equation of a curl-free electric field $\boldsymbol{E} = -\boldsymbol{\nabla}\phi$ generated by a cloud of static eletrons of density $-e(\boldsymbol{R})$ in a medium with a spatially varying dielectric constant $\epsilon(E)$ if we map the field $\boldsymbol{g} \leftarrow \boldsymbol{E}$, the density $\rho(\boldsymbol{R}) \leftarrow e(\boldsymbol{R})$ and the factor $\frac{\mu(g)}{G} \leftarrow \epsilon(E)$. The above modified Poisson's equation is actually a reformat of the Lagrange equation $\frac{\partial L}{\partial \Phi} = -\boldsymbol{\nabla}\cdot\frac{\partial L}{\partial \boldsymbol{g}}$, where the Lagrangian is given by

$$-L = \int \mathrm{d}\boldsymbol{R}^3\left[\rho\Phi + \frac{\bar{\mu}|\boldsymbol{g}|^2}{8\pi G}\right], \qquad \boldsymbol{g}(\boldsymbol{R}) = -\boldsymbol{\nabla}\Phi(\boldsymbol{R}), \tag{2}$$

where we integrate over the source energy density plus the field energy density; the factor $\bar{\mu}(g) \equiv \frac{\int \mu(g)\mathrm{d}(g^2)}{g^2}$. This classical field theory formulation guarantees conservations of energy and (angular) momentum of an isolated system.

In the past this non-relativistic formulation of MOND has been criticized for being incomplete for modelling the bending of light (but see Qin et al. 1995). This, too, has changed since its generalization into a respectable relativistic theory (christened TeVeS by Bekenstein 2004), which includes Hubble expansion, and passes standard tests to check General Relativity (Skordis et al. 2005; Chiu et al. 2005); GR is merely one limitting case of TeVeS.

⋆ PPARC Advanced Fellow.
⋆⋆ Outstanding Young Overseas Scholar.

Nevertheless, a main challenge of working on MOND is its essential subtle non-linearity and scale-dependency, which makes it unreliable to extrapolate Newtonian intuitions. As a result, there are very few predictions of MOND in the literature in dynamical situations where the non-sphericity of the potential is essential. It is encouraging that the recent work of Ciotti & Binney (2004) shows surprisingly simple analytical scaling relations exist even for the highly non-linear and non-spherical two-body relaxation problem in MOND. Here we show a surprisingly simple scaling of tides or the Roche lobe of a binary system (on either stellar or galaxy scales) if it is in the non-linear deep-MOND regime. A subtle difference from a naive Newtonian extrapolation is also pointed out. We compare the predicted Roche lobe sizes with the observed limiting sizes of Milky Way satellites (globular clusters and dwarf galaxies) of $10^{5-6.5}\ L_\odot$.

2. Roche lobe & binary potential in deep-MOND

One way to reach the deep-MOND regime so that $\mu(g)=\frac{g}{a_0}$ is to be at a distance R sufficiently far way from an isolated galaxy of total baryonic mass M so that the gravity $g(R)\ll a_0$. Here $g(R)$ and the spherical galaxy potential $\Phi_0(R)$ are approximately related to the Newtonian gravity GM/R^2 by

$$g(R)=\frac{\mathrm{d}\Phi_0(R)}{R}=\sqrt{\frac{GMa_0}{R^2}},\quad R\equiv\sqrt{z^2+y^2+x^2}. \tag{3}$$

Consider introducing a low-mass satellite of mass m at a position $(x,y,z)=(0,0,D_\mathrm{o})$ in the above galactic potential $\Phi_0(R)$. Following Milgrom (1986), we consider the effect of the self-gravity of a satellite mass inside an external galaxy field $g(R)\sim\sqrt{\frac{GMa_0}{R^2}}$. The spatially slow-varying external field dominates the satellite gravity sufficiently far away from the satellite. So the MOND "dielectric index" $\mu\sim\mu(g)\sim g(R)/a_0\sim\sqrt{\frac{GM}{a_0R^2}}$ varies very little in the vicinity of the satellite. To the first order in m the perturbation in potential is given by

$$\Phi_1(x,y,z)=-\frac{Gm'}{\tilde r},\quad m'\equiv\frac{m}{\mu(g_{D_\mathrm{o}})}, \tag{4}$$

where m' is the modified inertia of the satellite due to the external field $g_{D_\mathrm{o}}=g(D_\mathrm{o})$, and $\tilde r$ is the effective distance from the centre of the satellite given by

$$\tilde r=\sqrt{(z-D_\mathrm{o})^2+(y^2+x^2)\,(1+\Delta)},\quad \Delta\equiv\left.\frac{\mathrm{d}\ln\mu}{\mathrm{d}\ln g}\right|_{g=g(D_\mathrm{o})} \tag{5}$$

where $1+\Delta(g)$ is a shape factor[1]; clearly $1+\Delta(g)=2$ in the deep-MOND regime where $\mu\sim g/a_0$, and $1+\Delta(g)=1$ for strong gravity.

The above formulation allows us to approximate the potential of, e.g., the Milky Way galaxy with a satellite. Substitute in the expressions for μ, $g(R)$, R and $\tilde r$, the combined potential is then given by

$$\Phi=\Phi_0(R)+\Phi_1=(GMa_0)^{\frac12}\ln\sqrt{z^2+y^2+x^2}-\frac{Gm'}{\tilde r}, \tag{6}$$

which is an axisymmetric prolate potential with two centres separated by distance D_o along the z-axis, where the two terms represent the MONDian potential of the Milky Way and perturbation due to the satellite; here

$$m'=m\sqrt{\frac{D_\mathrm{o}^2a_0}{GM}},\qquad \tilde r=\sqrt{(z-D_\mathrm{o})^2+2y^2+2x^2}. \tag{7}$$

We also note that the density $\rho=0$ along the z-axis for the gravity field $\boldsymbol{g}=-\boldsymbol{\nabla}\Phi$ of the above combined potential; this can be verified by evaluating the modified Poisson's equation $\rho=-\boldsymbol{\nabla}\cdot\frac{\boldsymbol{g}\mu}{4\pi G}$.

Let the low-mass satellite with $m/M\ll1$ rotate around the galaxy centre (fixed) with an angular velocity $\Omega_0\hat{\boldsymbol{y}}$, then particles in the corotating frame conserve the Jacobi energy with an effective (triaxial) potential

$$\Phi_\mathrm{e}(x,y,z)\equiv\Phi(x,y,z)-\frac{x^2+z^2}{2}\Omega_0^2,\quad \Omega_0=\frac{\sqrt{GMa_0}}{D_\mathrm{o}}. \tag{8}$$

The inner or outer Lagrangian points is then calculated from the saddle point of the effective potential where

$$\left.\frac{\partial\Phi_\mathrm{e}(0,0,z)}{\partial z}\right|_{z=D_\mathrm{o}\pm r_\mathrm{L}}=0=\frac{\sqrt{GMa_0}}{D_\mathrm{o}\pm r_\mathrm{L}}\pm\frac{Gm'}{r_\mathrm{L}^2}-\Omega_0^2(D_\mathrm{o}\pm r_\mathrm{L}) \tag{9}$$

which defines the Lagrange radius r_L. Taylor-expand the above to first order in $r_\mathrm{L}/D_\mathrm{o}$ (the 0th term cancels due to Eqs. (8) and (7)), we have

$$\left(\frac{m}{r_\mathrm{L}^3}\right)\left(\frac{M}{D_\mathrm{o}^3}\right)^{-1}=1+\zeta\equiv\left[1+\frac{\Omega_0^2D_\mathrm{o}^2}{\sqrt{GMa_0}}\right]=2. \tag{10}$$

So inside the Lagrange radius the average density of the satellite equals twice the average density inside the orbit of the satellite in the weak gravity regime. Note that the masses here m and M are true baryonic masses of the binary, *not* the modified inertia masses[2]. The scaling that $r\propto m^{1/3}$ is also confirmed by the numerical simulations of Brada & Milgrom (2000).

The shape of the Roche lobe is defined by the contour of the effective potential (Eq. (8)) passing through the Lagrange point. Finding the roots analytically yields (Zhao & Tian 2005)

$$r=\left[1,\frac{\sqrt2}{3},(\sqrt{10}+\sqrt2)^{\frac13}-(\sqrt{10}-\sqrt2)^{\frac13}\right]\left(\frac{m}{2M}\right)^{\frac13}D_\mathrm{o}, \tag{11}$$

which are intersections with the long z-axis, intermediate x-axis and rotation y-axis respectively. Of the three radii, the Intermediate Roche (IR) radius compares most directly with observed size in the sky plane for a distant satellite, and is given by

$$\frac{r_\mathrm{IR}}{D_\mathrm{o}}\left(\frac{m}{M}\right)^{-\frac13}=\frac{\sqrt2}{3}\left(\frac12\right)^{\frac13}=0.374. \tag{12}$$

[1] The "dielectric index" $\mu(\frac{|\boldsymbol{g}|}{a})$ is more sensitive to perturbation along the external field $g(D_\mathrm{o})\hat{\boldsymbol{z}}$ direction than perpendicular because $|\boldsymbol{g}+\mathrm{d}\boldsymbol{g}|=\left[(g_{D_\mathrm{o}}+\mathrm{d}g_z)^2+(\mathrm{d}g_x)^2+(\mathrm{d}g_y)^2\right]^{\frac12}$ depends on the perturbation $\mathrm{d}g_z$ to first order, and $\mathrm{d}g_x$ and $\mathrm{d}g_y$ to second order.

[2] Dimensional analysis only cannot tell whether the dimensionless $\frac{r_\mathrm{L}}{D_\mathrm{o}}$ scales like $\left(\frac{m}{M}\right)^n$ or $\left(\frac{m'}{M}\right)^n$, where $m'=\frac{m}{\mu}$ is the modified inertia (cf. Eq. (4)).

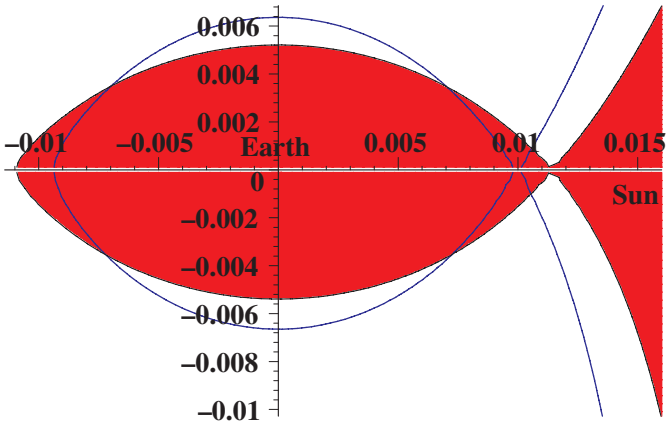

Fig. 1. shows the re-scaled Roche lobes (contours of the effective potential) in the equatorial xz plane (*lower half*) and in the vertical yz plane (*upper half*) of a hypothetical isolated Earth-Sun binary with a mass ratio 3×10^{-6} in the strong gravity regime (say with the separation $D_{\rm o}=1$ AU, thin blue lines), and in the weak gravity regime (say with separation $D_{\rm o}=0.1$ pc and $GM_\odot D_{\rm o}^{-2}a_0^{-1}\sim0.1$, shaded areas). The Earth is at origin and the Sun is at unit length to the right. The inner Lagrangian point is a saddle point between the Earth and the Sun, which is slightly further away from the Earth in the deep-MOND regime than in strong gravity regime.

Projection effects make the observed radius in between the short semi-axis and the long semi-axis of the Roche lobe. Hence the intermediate axis ($r_{\rm IR}$ instead of $r_{\rm L}$) is the best compromise among the three to approximates the observed size.

3. Observed instantaneous Roche lobe

If MOND is correct the Roche lobe would act as Nature's balance to weigh the relative baryonic content of a secondary vs. a primary star, or a satellite vs. its host galaxy. Interestingly the Roche lobe satisfies the same scaling relation $\frac{r_{\rm IR}}{D_{\rm o}}\left(\frac{m}{M}\right)^{-1/3}=$ cst, but the cst $=0.462$ in strong gravity regime (Binney & Tremaine 1987) while cst $=0.374$ in deep-MOND. E.g., in a gedanke experiment where we take the solar system out of the Galaxy, and increase the Earth-Sun distance from 1AU to 0.1 pc (the separation of the widest known binary stars) so that near the inner Lagrangian point of the system the gravity drops from the strong regime to the weak regime. Fixing the Earth-Sun mass ratio $m/M=3\times10^{-6}$, the rescaled intermediate Roche lobe radius $r_{\rm IR}/l$ should decreases slowly by a subtle amount from $0.462\times(m/M)^{1/3}=0.0067$ radian (for strong gravity) to $0.374\times(m/M)^{1/3}=0.0054$ radian (for weak gravity); cf. Eqs. (10) and (12) and see Fig. 1. Likewise the aspect ratios of the Roche lobe evolves from $1{:}2/3{:}9^{1/3}{-}3^{1/3}=1{:}0.667{:}0.638$ (Binney & Tremaine 1986) to about 1:0.471:0.456, and the volume of Roche lobe evolves from $\sim\frac{4\pi D_{\rm o}^3}{3}\frac{m}{7M}$ to $\sim\frac{4\pi D_{\rm o}^3}{3}\frac{m}{9M}$. The Roche lobe is more squashed in MOND than in Newtonian gravity (cf. Fig. 1).

Interestingly, the same rescaled Roche radius can be predicted if we substitute the Earth-Sun binary by a satellite (either a dwarf spheroidal or a globular cluster) of a typical luminosity $\sim3\times10^5\ L_\odot$ orbiting a luminous host galaxy of $\sim10^{11}\ L_\odot$ so that the baryonic mass ratio is about Earth-Sun mass ratio. The self-gravity around an extended object of mass distribution $m(r)$ becomes weak compared to a_0 outside a radius

$$r^{\rm w}=\sqrt{\frac{Gm(r)}{a_0}}=\begin{cases}0.1\ {\rm pc} & m=10\ M_\odot,\\ 10\ {\rm pc} & m=10^5\ M_\odot,\\ 10^4\ {\rm pc} & m=10^{11}\ M_\odot.\end{cases}\qquad(13)$$

Consider globular clusters and dwarf galaxies of the Milky Way much further than 10 kpc. The outer envelope (well outside 10 pc) of these objects are generally in *the mildly-weak to the deep-MOND regime*. A satellite is generally on a non-circular orbit, nevertheless, an instantaneous Roche lobe radius can still be defined by the $r_{\rm IR}$ as if the satellite is orbiting on a circular orbit at its present orbital radius $D_{\rm o}$ (approximately the distance from the Sun D) for an outer halo satellite. So we can rewrite Eq. (12) as

$$\frac{r_{\rm IR}}{D}=A\left(\frac{L_{\rm sat}}{L_{\rm MW}}\right)^{\frac{1}{3}},\qquad A\equiv0.374\frac{D_{\rm o}}{D}\sim0.374,\qquad(14)$$

where in estimating the instantaneous Roche radius $r_{\rm IR}$ (cf. Eq. (12)) we have assumed satellites have identical mass-to-light ratio as the Milky Way. This suggests comparable sizes $r_{\rm IR}$ for distant satellites at similar present distances D or $D_{\rm o}$ and comparable luminosity $L_{\rm sat}$.

The actual direct observable is the limiting angular size $\theta_{\rm lim}$ of a satellite seen from the Sun's perspective. If a satellite fills the MONDian Instantaneous Roche Lobe, we expect to observe an angular size $\theta_{\rm lim}=r_{\rm IR}/D$ perpendicular to the line of sight. From these observables we can construct an observable "filling factor"

$$F_{\rm lim}\equiv\frac{\theta_{\rm lim}}{r_{\rm IR}/D}=\frac{\theta_{\rm lim}}{A}\left(\frac{L_{\rm sat}}{L_{\rm MW}}\right)^{-\frac{1}{3}}.\qquad(15)$$

In the real world, the limiting radius should be somewhat smaller than the instantaneous Roche radius, i.e., $F_{\rm lim}\leq1$ because (i) the satellite likely remembers the truncation set by the stronger tide at some smaller orbital radius between last pericentre $r_{\rm p}$ and present distance D, depending on whether a satellite can relax quickly in one orbital time (Bellazzini 2004); (ii) this truncation might be beyond the limit of reliable observation $r_{\rm lim}$ simply because we run out of bright stars (Grebel et al. 2000). Many satellites (cf. Dinescu et al. 2004, and references therein) are on nearly circular orbits (Ursa Minor and Canis Major dwarves) or are presently within a factor of two to their pericentres (Pal3, Pal13, Fornax, Sgr and LMC). Theoretically a particle is typically found at the geometric mean $\sqrt{r_{\rm p}r_{\rm a}}$ of its pericentre and apocentre in a logarithmic potential. So $D\sim D_{\rm o}\sim(1-2)r_{\rm p}$ typically even for a very radial orbit with $r_{\rm p}{:}r_{\rm a}\sim1{:}4$, i.e., we expect a mild scatter of $F_{\rm lim}$ between 0.5–1, allowing for radial orbits. The filling factor should be nearly unity for globular clusters since many galactic and some extragalactic globulars (Harris et al. 2002) apparently fill their Roche lobes judging from extra-tidal stars in power-law profiles revealed by deep observations wherever available (e.g., Leon et al. 1996).

These expectations, however, are not borne out by Fig. 2, which shows surprisingly large scatter of the observed $F_{\rm lim}\sim0.1{-}5$ for distant Milky Way satellites with comparable luminosities ($10^5{-}10^{6.5}\ L_\odot$). It is also difficult to understand why

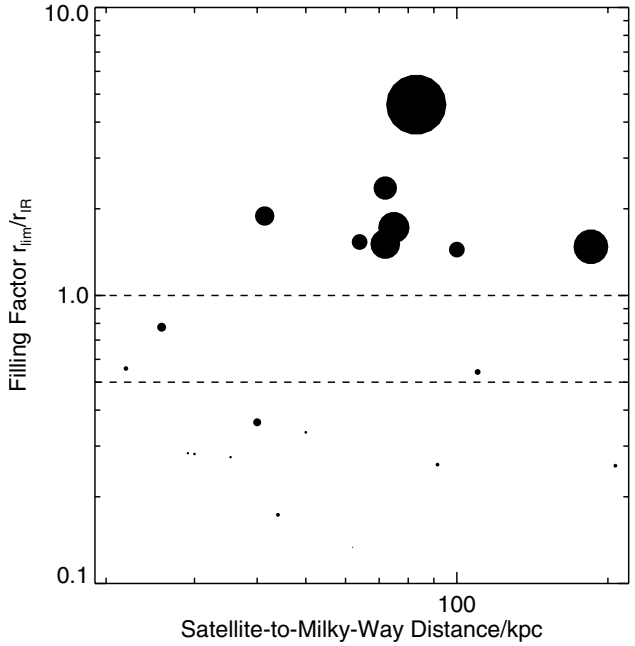

Fig. 2. shows the MONDian "filling factor" for outer Galactic satellites (20–200 kpc), i.e., the ratio of the observed limiting radius $r_{\rm lim}$ and the instantaneous Intermediate Roche radius $r_{\rm IR}$ (cf. Eq. (15), with a nominal luminosity $L_{\rm MW} = 4 \times 10^{10}\ L_\odot$ for the Galaxy). The overall distribution is much broader than the range expected in MOND (indicated between the two thick dashed lines), and many are outliers with $r_{\rm lim} > r_{\rm IR}$. The symbol sizes are proportional to the apparent limitting sizes $\frac{r_{\rm lim}}{D}$ of satellites (the smallest/biggest symbols correspond to physical radii of 40 pc/4000 pc, observational errors on distance and $\theta_{\rm lim}$ are 10% typically), and the sample includes both globular clusters and dwarf galaxies with luminosities between 10^5–$10^{6.5}\ L_\odot$ (data from Harris 1996; Mateo 1998).

our expectation $F_{\rm lim} \leq 1$ (cf. Eq. (15)) is contradicted most strikingly by systems of larger tidal radii (larger symbols). Surely observations carry errors. The distance factor A is insensitive to the typical 10% distance error. Satellites often change profiles at $\theta_{\rm lim}$, so $\theta_{\rm lim}$ is well-defined with very little error. Finally many satellites are in mild MOND regime with a Roche lobe size more rigorously given by (Zhao & Tian 2005)

$$\frac{\text{Intermediate Roche Size}}{\text{Orbital Radius}} = \frac{2}{3\sqrt{1+\Delta}} \left(\frac{1+\Delta}{3+\Delta}\frac{m}{M}\right)^{\frac{1}{3}}, \qquad (16)$$

which is a smooth interpolation of Eq. (12) in deep-MOND and the familiar Newtonian prediction (Binney & Tremaine 1987) as the dilation factor (cf. Eq. (5)) $1+\Delta(\frac{g}{a_0})$ changes from 2 to 1. For any μ-function of the Milky Way (cf. Zhao & Famaey 2005; Famaey & Binney 2005), this correction is at most only 20% (the factor 0.374 in Eq. (12) changed to 0.462).

In short, it is likely challenging for any theory of structure formation of a baryonic MOND universe to explain the puzzling large scatter in the rescaled Roche radius without fine-tuning of satellite orbits and mass-to-light ratios. It is less challenging for dark matter theories; 10^5-star satellite objects could form either inside or outside a small dark halo. The scatter of satellite sizes echos with similar scatter of Einstein ring sizes around high-redshift lens galaxies (see lensing models of Zhao et al. 2005), highlighting possible difficulties of mass-trace-light models.

Acknowledgements. H.S.Z. thanks the referee for constructive comments, LanLan Tian and Huanyuan Shan for help, and partial support from Chinese NSF grant 10428308.

References

Bekenstein, J. 2004, Phys. Rev. D, 70, 3509
Bekenstein, J., & Milgrom, M. 1984, ApJ, 286, 7
Bellazzini, M. 2004, MNRAS, 347, 119
Binney, J., & Tremaine, S. 1987, Galaxy dynamics, PUP
Brada, R., & Milgrom, M. 2000, ApJ, 541, 556
Chiu, M., Ko, C.-M., & Tian, Y. 2005, ApJ, in press
Ciotti, L., & Binney, J. 2004, MNRAS, 351, 285
Dinescu, D., Keeney, B. A., Majewski, S. R., & Girard, T. M. 2004, AJ, 128, 687
Famaey, B., & Binney, J. 2005, MNRAS, 363, 603
Grebel, E., Odenkirchen, M., & Harbeck, D. 2000, A&AS, 200, 4607
Harris, W. E. 1996, AJ, 112, 1487
Harris, W. E., Harris, G. L. H., Holland, S. T., & McLaughlin, D. E. 2002, AJ, 124, 1435
Leon, S., Meylan, G., & Combes, F. 2000, A&A, 359, 907
Mateo, M. 1998, ARA&A, 36, 435
Milgrom, M. 1983, ApJ, 270, 365
Milgrom, M. 1986, ApJ, 302, 617
Milgrom, M., & Sanders, R. H. 2003, ApJ, 599, L25,
Pointecouteau, E., & Silk, J. 2005, MNRAS, in press
Sanders, R., & McGaugh, S. 2002, ARA&A, 40, 263
Skordis, C., Mota, D. F., Ferreira, P. G., & Boehm, C. [arXiv:astro-ph/0505519]
Qin B., Wu X. P., Zou, L. Z., et al. 1995, A&A, 296, 264
Zhao, H., & Tian, L. 2005, A&A, submitted
Zhao, H. S., Bacon, D., Taylor, A. N., & Horne, K. D. 2005, MNRAS submitted [arXiv:astro-ph/0509590]
Zhao, H. S., & Famaey, B. 2005, ApJ, submitted